Novel Photoanode Structure Templated from Butterfly Wing Scales

Wang Zhang,[†] Di Zhang,[*,†] Tongxiang Fan,[†] Jiajun Gu,[†] Jian Ding,[†] Hao Wang,[‡] Qixin Guo,[§] and Hiroshi Ogawa[§]

State Key Laboratory of Metal Matrix Composites, Shanghai Jiao Tong University, 200240 Shanghai, P.R. China, University of Michigan−Shanghai Jiao Tong University Joint Institute, and Department of Electrical and Electronic Engineering, Saga University, Saga 840-8502, Japan

Received July 11, 2007. Revised Manuscript Received October 16, 2008

We studied a novel photoanode structure inspired by butterfly wing scales with potential application on dye-sensitized solar cell in this paper. Quasi-honeycomb like structure (QHS), shallow concavities structure (SCS), and cross-ribbing structure (CRS) were synthesized onto a fluorine-doped tin-oxide-coated glass substrate using butterfly wings as biotemplates separately. Morphologies of the photoanodes, which were maintained from the original butterfly wings, were characterized by scanning and transmission electron microscopies. The results show that the calcined photoanodes with butterfly wings' structures, which comprised arranged ridges and ribs consisting of nanoparticles, were fully crystallined. Analysis of absorption spectra measurements under visible light wavelength indicates that the light-harvesting efficiencies of the QHS photoanode were higher than the normal titania photoanode without biotemplates because of the special microstructures, and then the whole solar cell efficiency can be lifted based on this.

Introduction

The dye-sensitized solar cell (also know as the photoelectrochemical Grätzel Cell) was first reported by Dr. Michael Grätzel and his group (École Polytechnique Fédérale de Lausanne, Switzerland) in 1991.[1] The cell consists of a dye-adsorbed mesoporous titania film filled with iodide/triiodide redox electrolyte and a Pt or carbon counter photoanode. Studies show that there are many factors limiting the cell whole performance. Many works have been directed toward improving the efficiency of dye-sensitized solar cells (DSC) by developing new dyes, suppressing charge recombination, or improving the properties of photoanodes. The properties of the photoanode have crucial influences on the light harvesting efficiency, which influences the whole cell efficiency of the DSC. As such, more and more efforts have been directed toward improving the performance of DSC through the optimization and treatment of titania photoelectrodes. To improve the photoanode characteristics, especially the light harvesting efficiency, researchers are studying different aspects such as crystal phase and size, doping methods, optimized materials, and proper structures. Recently, many works have been done to enhance the optical path length of the photoanodes by tuning the film morphology, such as taking hollow sphere voids and solid particles with large size as scattering centers[2,3] amd coupling a photonic crystal layer[4,5] or a multilayer structure[6] on the surface of the photoanode. With the increase in the optical path length, the light absorption efficiency will increase at the same time. Consequently, developing a light trapping model[7] that can enhance the optical path length via the new structural materials is a very effective approach to achieve better light-collection effects. Furthermore, the increase of the path length of the photons inside DSC will increase the probability of interacting with dye molecules; it is very important to scatter incident light.[8] The increased amount of light-scattering particles and the scattering center gradient may account for the enhanced photon-to-current efficiencies.[9]

Recently, discoveries on butterfly wings show that some microstructures on the wings surface are effective solar collectors[10] or blocks.[11] They measured the reflectance of light at normal incidence and reflection directions and compared this to the predictions of a model, which assumes that the reflection is due to alternating layers of air and chitin. It suggested that the solar heat is absorbed and conducted away by the ridges or ribs in the wing. Because it can absorb more heat at faster rapid, it could increase the individuals' body temperatures faster and plentier. This mechanism could enhance the survival chances of the butterfly individuals in

* Corresponding author. Fax: 86-021-3420 2749. Tel: 86-021-3420 2634. E-mail: zhangdi@sjtu.edu.cn.
† Shanghai Jiao Tong University.
‡ University of Michigan−Shanghai Jiao Tong University Joint Institute.
§ Saga University.

(1) Grätzel, M. *Nature* **2001**, *414*, 338, and references therein.
(2) Barbe, C. J.; Arendse, F.; Comte, P.; Jirousek, M.; Lenzmann, F.; -Shklover, V.; Grätzel, M. *J. Am. Ceram. Soc.* **1997**, *80*, 3157.
(3) Hore, S.; Nitz, P.; Vetter, C.; Prahl, C.; Niggemann, M.; Kern, R. *Chem. Commun.* **2005**, 2011.
(4) Nishimura, S.; Abrams, N.; Lewis, B. A.; Halaoui, L. I.; Mallouk, T. E.; Benkstein, K. D.; van de Lagemaat, J.; Frank, A. J. *J. Am. Chem. Soc.* **2003**, *125*, 6306.
(5) Chen, I. L.; Freymann, G.; Choi, S. Y.; Kitaev, V.; Ozin, G. A. *J. Mater. Chem.* **2008**, *18*, 369.
(6) Wang, Z. S.; Kawauchi, H.; Kashima, T.; Arakawa, H. *Coord. Chem. Rev.* **2004**, *248*, 1381.
(7) Vargas, W. E.; Niklasson, G. A. *Sol. Energy Mater. Sol. Cells* **2001**, *69*, 147.
(8) Horea, S.; Vetterb, C.; Kerna, R.; Smitc, H.; Hinsch, A. *Sol. Energy Mater. Sol. Cells* **2006**, *90*, 1176.
(9) Wang, Z. S.; Yanagida, M.; Sayama, K.; Sugihara, H. *Chem. Mater.* **2006**, *18*, 2912.
(10) Heilman, B. D.; Miaoulis, I. N. *Appl. Opt.* **1994**, *33*, 6642.
(11) Koon, D. W.; Crawford, A. B. *Appl. Opt.* **2000**, *39*, 2496.

10.1021/cm702458p CCC: $40.75
Published on Web 12/15/2008

Scheme 1. Schematic Illustrations for the Transition Process of Butterfly Wings onto the FTO Glass Slices: Step 1, Soak the Butterfly Wings in the Titanium Sulfate Precursor; Step 2, Calcine the Soaked Butterfly Wings onto the Prepared Anatase Film on the FTO; Simplified Configuration of the As-Synthesized Quasi-Honeycomb Structure Photoanode Shown on the Right

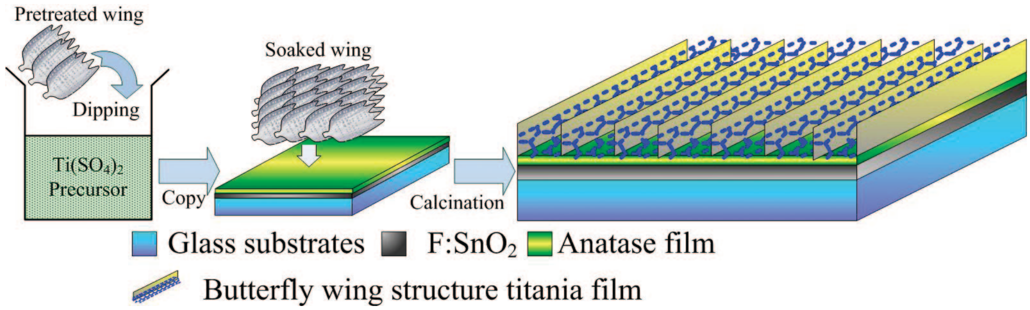

cold climates or high-altitude areas. More excitingly, scientists[12] found that scales with the honeycomb structure were on average significantly less reflective than those with cross-ribbing structure. The honeycomb-like pattern scales take advantage of refraction on trapping light, much like a fiber-optic cable. The scales on the wings have a relatively high refractive index, so they take advantage of total internal reflection. That is, the light enters the material, but whenever the light meets another part of the surface, instead of crossing, it is reflected back into the material. So nearly all the incident light could be adsorpted. A series of experiment results show that the honeycomb microstructure scales are more effective in minimizing surface reflections and increasing optical path length than the wings with other two microstructures studied in this work. Inspired by this, here we present a butterfly wing scales microstructure titania film photoanode and illustrate how this topology could improve the light absorptivity and specific surface area of the DSC photoanode.

To prepare the titania mesoporous film photoanodes, researchers utilize many methods, such as doctor blade deposition, layer by layer deposition, electro deposition, spraying pyrolysis deposition, screen printing, and so on.[13−15] In this work, to maintain the butterfly wings' microstructure into the photoanode film intact and correctly, we adopted an improved biotemplate method. This method, which can combine the merits offered by both the material and biological structures for fabricating unique structures with much enhanced mechanical properties and finely tuned optical performance, gained great development in recent years. Nowadays, a variety of biological species with a variety of unique microstructures, including bacteria[16] and fungal colonies,[17] wood cell,[18] diatoms,[19] echinoid skeletal plates,[20] pollen grains,[21] eggshell membranes,[22] silk,[23] and so on, have been used as templates to fabricate complex inorganic structures for different potential applications. Allured by butterfly wings special and complex hierarchical microstructures, many groups[24] including ours[25] have dedicated thenselves to studying on the transformation and characteristics of the inorganic butterfly wings. These works studied the different potential applications of the butterfly wings' structures with different components. By modifying the method we used before, the butterfly wing microstructures were inherited into the photoanode titania film successfully. The properties of the photoanodes are also discussed.

Experimental Section

Wings taken from two species of butterfly were used as biotemplate in our work, one is *Papilio paris* Linnaeus (subfamily *Papilionidae* of the family *Nymphalidae*), the other is *Thaumantis diores* (Doubleday) (subfamily *Amathusiidae* of the family *Nymphalidae*); both of them were kindly supplied by Shanghai Natural Wild-Insect Kingdom Co., Ltd.

Analytic grade reagents HCl, NaOH, $Ti(SO_4)_2 \cdot 4H_2O$, isopropanol $((CH_3)_2CHOH)_2$, CCl_4, absolute alcohol, and deionized water were provided by Shanghai Chemical Company. An electrically conducting Fluorine-doped Tin Oxide (FTO) coated glass (20 Ω/sq, Qinhuangdao YaoHua Glass Co.,Ltd.) was used as substrate. The FTO glass was cleaned in deionized water with ultrasonication for 5 min. It was then hydroxylated by ultrasonication for 3 min in a mixture of 60 mL of isopropanol and 40 mL of aqueous KOH with concentration of 1 M, followed by rinsing in deionized water with sonication for 10 min. After these cleaning procedures, the surface of substrates became hydrophilic. It can be anticipated that the hydrophilic FTO glass is suitable for covering a layer of TiO_2 film.

Titanium sulfate was dissolved in absolute alcohol with different concentrations. After the solution was stirred for 1 h at 60 °C, the pH was adjusted to the range of 2.5−3.0 by adding dilute H_2SO_4. An appropriate amount of nonionic surfactant Triton X100 was also added to this solution. Butterfly wings were pretreated in advance to remove salts and proteins. Then the pretreated butterfly wings were immersed into the titanium sulfate precursor solution main-

(12) Vukusic, P.; Sambles, J. R.; Lawrence, C. R. *Proc. R. Soc. London, B* **2004**, *271*, S237.
(13) Kumara, G. R. R. A.; Konno, A.; Senadeera, G. K. R.; Jayaweera, P. V. V.; de Silva, D. B. R. A.; Tennakone, K. *Sol. Energy Mater Sol. Cells* **2001**, *69*, 195.
(14) Choy, K. L.; Su, B. J. *Mater. Sci. Lett.* **1999**, *18*, 943.
(15) Okuya, M.; Nakade, K.; Osa, D.; Nakano, T.; Kumara, G. R. R. A.; Kaneko, S. *J. Photochem. Photobiol. A: Chem.* **2004**, *164*, 167.
(16) (a) Davis, S. A.; Burkett, S. L.; Mendelson, N. H.; Mann, S. *Nature* **1997**, *385*, 420. (b) Zhang, B.-J.; Davis, S. A.; Mendelson, N. H.; Mann, S. *Chem. Commun.* **2000**, 781. (c) Zhou, H.; Fan, T. X.; Zhang, D. *Chem. Mater.* **2007**, *19*, 2144.
(17) Li, Z.; Chung, S.-W.; Nam, J.-M.; Ginger, D. S.; Mirkin, C. A. *Angew. Chem., Int. Ed.* **2003**, *42*, 2306.
(18) (a) Wang, Dong, Y.; Tang, Y.; Ren, N.; Zhang, Y.; Yue, Y.; Gao, Z. *Adv. Mater.* **2002**, *14*, 926. (b) Sun, B. H.; Fan, T. X.; Zhang, D.; Okabe, T. *Carbon* **2004**, *42*, 177.
(19) (a) Anderson, M. W.; Holmes, S. M.; Hanif, N.; Cundy, C. S. *Angew. Chem., Int. Ed.* **2000**, *39*, 2707. (b) Wang, Y.; Tang, Y.; Dong, A.; Wang, X.; Ren, N.; Gao, Z. *J. Mater. Chem.* **2002**, *12*, 1812.
(20) Meldrum, F. C.; Seshadri, R. *Chem. Commun.* **2000**, *1*, 29.
(21) Hall, S. R.; Bolger, H.; Mann, S. *Chem. Commun.* **2003**, *22*, 2784.
(22) (a) Yang, D.; Qi, L. M.; Ma, J. M. *Adv. Mater.* **2002**, *14*, 1543. (b) Dong, Q.; Su, H. L.; Zhang, D.; Zhang, F. Y. *Nanotechnology* **2006**, *17*, 3968.
(23) He, J.; Kunitake, T. *Chem. Mater.* **2004**, *16*, 2656.

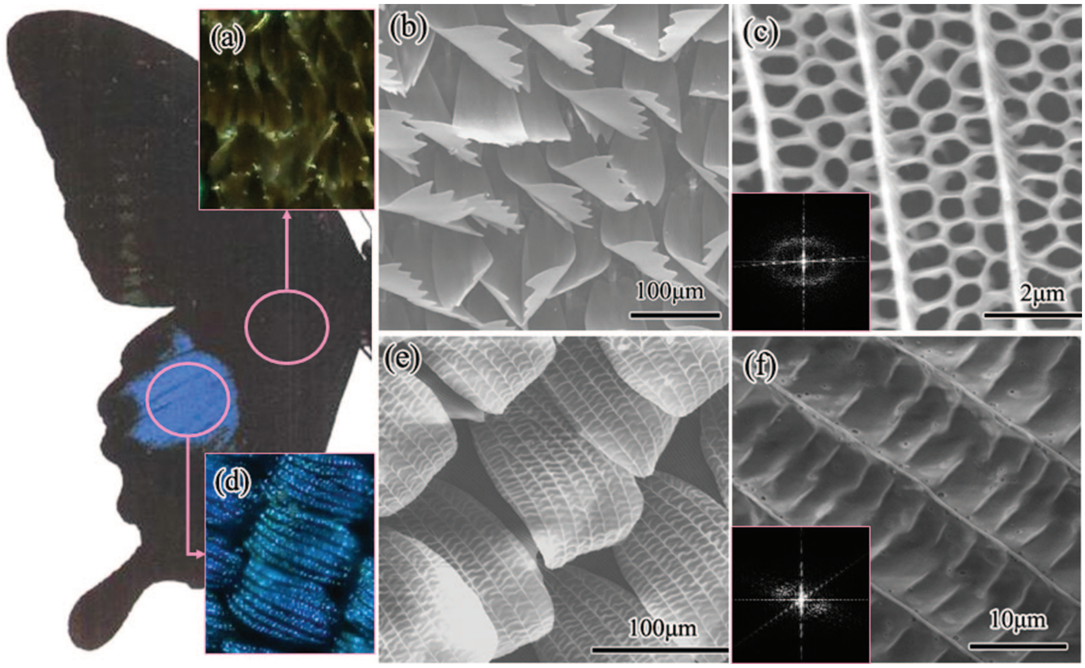

Figure 1. Nature picture and low-magnification optical microscopy, low-magnification FESEM images and high-resolution FESEM images showing the wing of the blue male (a−c) and black male (d−f). The insets in the lower left-hand (c, f) corner show the two-dimensional, logarithmic Fourier power spectra of square areas selected from the images.

Table 1. Measurements and statistical Data of the Quasi-Honeycomb Structure and Cross-Ribbing Structure before and after Calcination As Calculated from FESEM Images Shown in Figures and and S3 Using IPP Software[a]

sample	mean hole diameter (μm)	mean hole area (μm^2)	total hole area (μm^2)	total area (μm^2)	fill factor (hole)
QHS (Original)	0.364	0.118	16.659	45.92	0.363
QHS-1 (Replica)	0.263	0.061	8.881	28.13	0.316
QHS-2 (Replica)			3.590	50.62	0.071
CRS (Original)	0.502	0.220	16.021	29.02	0.552
CRS (Replica)	0.522	0.209	39.612	74.52	0.532

[a] QHS-1, the true replica of the quasi-honeycomb structure butterfly wing; QHS-2, the fulfilled titania replica; CRS (Original) & CRS(Replica): shown in the Supporting Information, a and b in Figure S3).

tained at constant temperature over 60 °C for 24 h or more, and then removed from the precursor solution, rinsed thoroughly with absolute alcohol. At first, we prepared a layer of colloidal TiO_2 dispersed on the FTO conductive surface, which was analogous to the method reported by Grätzel and co-workers.[1,26] The immerged wing scales were then subsequently placed on the layer of the colloidal TiO_2 film, covered by another piece of FTO glass. Two pieces of the FTO glasses were tightly clamped, as to keep the soaked wings flat and improve the interface between colloidal TiO_2 film layer and soaked biotemplates.

At last, the specimen was then placed into an oven, and was heated up to 500 °C with the slow heating rate at 1 °C/min in air. The slow heating rate was adopted so that to avoid the appearance of cracks and frame collapse of the soaked wings during sintering process. By keeping the specimen inside for 2 h with such temperature, the chitinous substrates were removed completely after reaction with air, leaving only TiO_2 in the form of ceramic butterfly wings. Then, the as-prepared “butterfly wing microstructure photoanode” was thus obtained. Scheme 1 shows the schematic illustrations of the transition process of butterfly wings onto the FTO glass slices. A simplified sketch of the as-synthesized butterfly wing microstructure photoanode is shown on the right side of Scheme 1. The as-synthesized photoanodes are divided into four layers: glass substrates, $F:SnO_2$ conductive layer, anatase film, and titania film with butterfly wing microstructures.

Digital microscope (Keyence VHX 100) was used to observe the low magnification morphologies of the original butterfly wing scales. The investigation of morphologies and microstructures of the original butterfly wings and as-made photoanode were carried out by field-emission scanning electron microscope (FESEM, FEI XL30). Investigation of original butterfly wings’ chemical composition was taken by energy-dispersive X-ray spectroscopy (EDXS) microanalysis (JED2300) attached to JEOL JSM-6360LV SEM. The microstructures and components of the as-synthesized titania film were analyzed in FESEM (FEI XL30) attached with EDXS (INCA OXFORD). Measurements, statistics and fast Fourier transform of the images are executed by using Image Pro Plus (IPP, version 6.0, Media Cybernetics, Silver Spring, MD). Absorbance spectra were recorded with a Varian Cary 500 UV−vis−NIR spectrophotometer by using a solid sample holder attachment. The TEM observation was performed in a JEOL 2010 type transmission electron microscope operated at 200 kV. Nitrogen adsorption−desorption isotherms were measured with a Micromeritics ASAP 2020 adsorption analyzer (Micromeritics Instrument Corp., Norcross, GA). The electrical conductivities were determined on CHI760C electrochemical analyzer (CH Instruments Corp. USA) in a three-electrode configuration, with a platinum counter electrode and Ag/AgCl reference electrode. The electrolyte used is 3.5% NaCl water solution at room temperature. The scanning rate was 1mV/s.

(24) (a) Cook, G.; Timms, P. L.; Spickermann, C. G. *Angew. Chem., Int. Ed.* **2003**, *42*, 557. (b) Silver, J.; Withnall, R.; Ireland, T. G.; Fern, G. R. *J. Mod. Opt.* **2005**, *52*, 999. (c) Li, B.; Zhou, J.; Zong, R. L.; Fu, M.; Bai, Y.; Li, L. T.; Li, Q. *J. Am. Ceram. Soc.* **2006**, *89*, 2298. (d) Zhang, J. Z.; Gu, Z. Z.; Chen, H. H.; Fujishima, A.; Sato, O. *J. Nanosci. Nanotechnol.* **2006**, *6*, 1173. (e) Y Huang, J.; Wang, X. D.; Wang, Z. L. *Nano lett.* **2006**, *6*, 2325.
(25) (a) Zhang, W.; Zhang, D.; Fan, T. X.; Ding, J.; Guo, Q. X.; Ogawa, H. *Nanotechnology* **2006**, *17*, 840. (b) Zhang, W.; Zhang, D.; Fan, T. X.; Ding, J.; Guo, Q. X.; Ogawa, H. *Microporous Mesoporous Mater.* **2006**, *92*, 227. (c) Zhang, W.; Zhang, D.; Fan, T. X.; Ding, J.; Guo, Q. X.; Ogawa, H. *Bioinspiration Biomimetics* **2006**, *1*, 89.
(26) Huang, S. Y.; Schlichthörl, G.; Nozik, A. J.; Grätzel, M.; Frank, A. J. *J. Phys. Chem. B* **1997**, *101*, 2576.

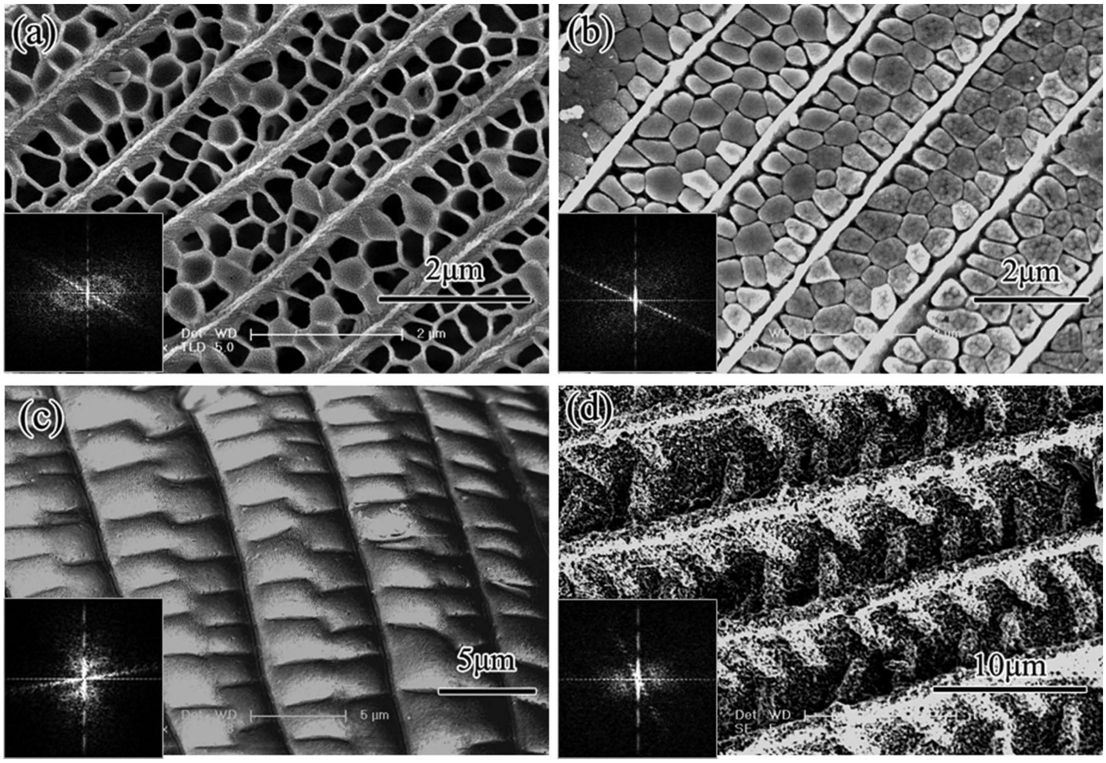

Figure 2. FESEM images of as-synthesized titania photoanodes templated from butterfly wings with different colors. (a, b) Quasi-beehive structures synthesized in different conditions; (c, d) shallow concavities structures in different conditions.

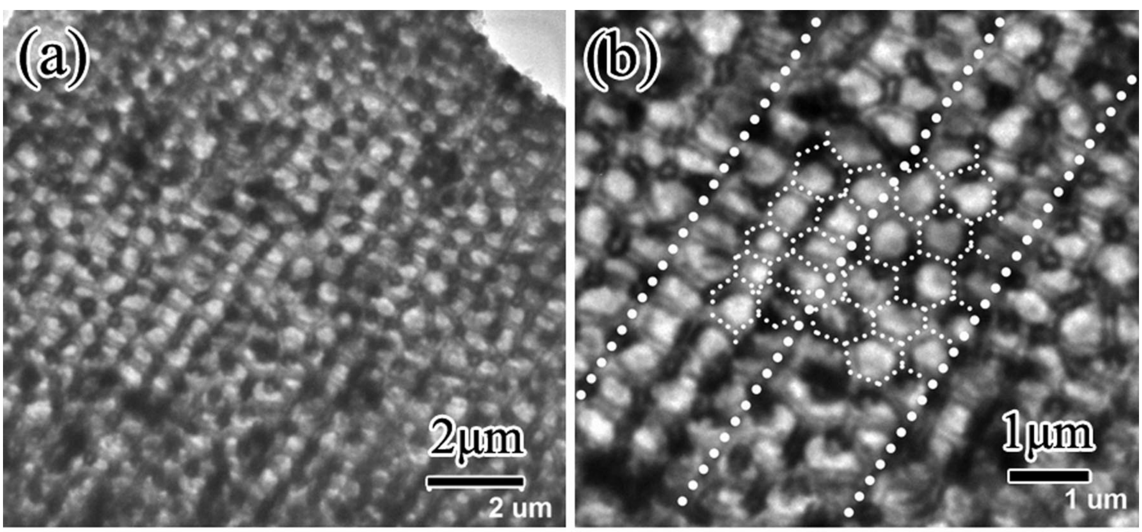

Figure 3. Medium- and high-resolution transmission electron microscopy images of quasi-honeycomb structure titania film. The dotted line delineated the quasi-honeycomb structure legibly in b.

The mercury intrusion measurements were performed with a Micromeritics PoreSizer 9320.

Results and Discussion

Papilio paris is a species of beautiful swallowtail butterfly found in South China. Expanse of the wings is about 100 mm. Upperside of the wings is black, irrorated with dark green scales, which on the outer portion of the forewing coalesce and form an incomplete post discal narrow band. On the hind wing, there is a conspicuous upper discal shining blue patch. The other specie of butterfly used in our work as contrast is *Thaumantis diores*, the upper wings of which are brown black. All the wings were scissored into 1 cm × 1 cm square samples from different colors.

A four-level observation method[27] was adopted in studying the morphology of butterfly wings. The first level deals with the macroscopic aspect of the butterfly wings, as the left

(27) S. Berthier, *Les Couleurs des Papillons*; Springer-Verlag: Paris, 2000.

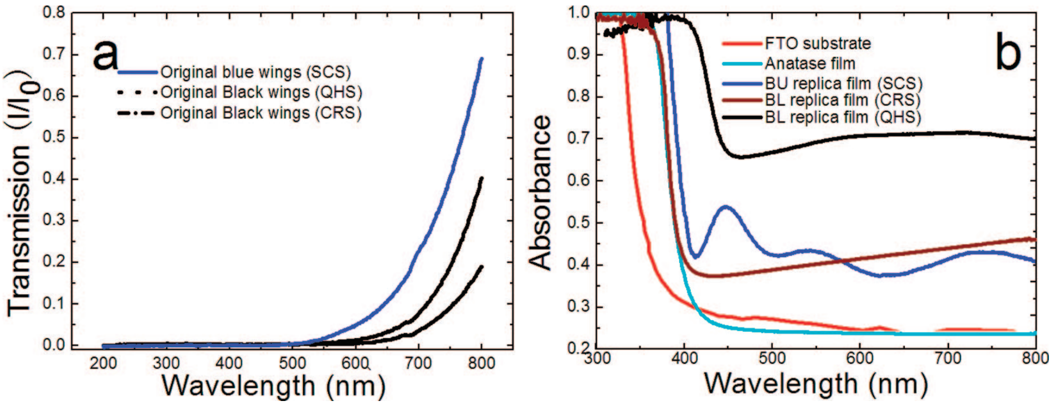

Figure 4. (a) Transmission spectra of the original butterfly wings: Continuous line (blue), short dash dot line (black wings with cross-ribbing structure), dot line (black wings with quasi-honeycomb structure). (b) The wavelength-dependent absorption (at normal incidence). Different colors represent different samples (cutline shown in the upper right corner).

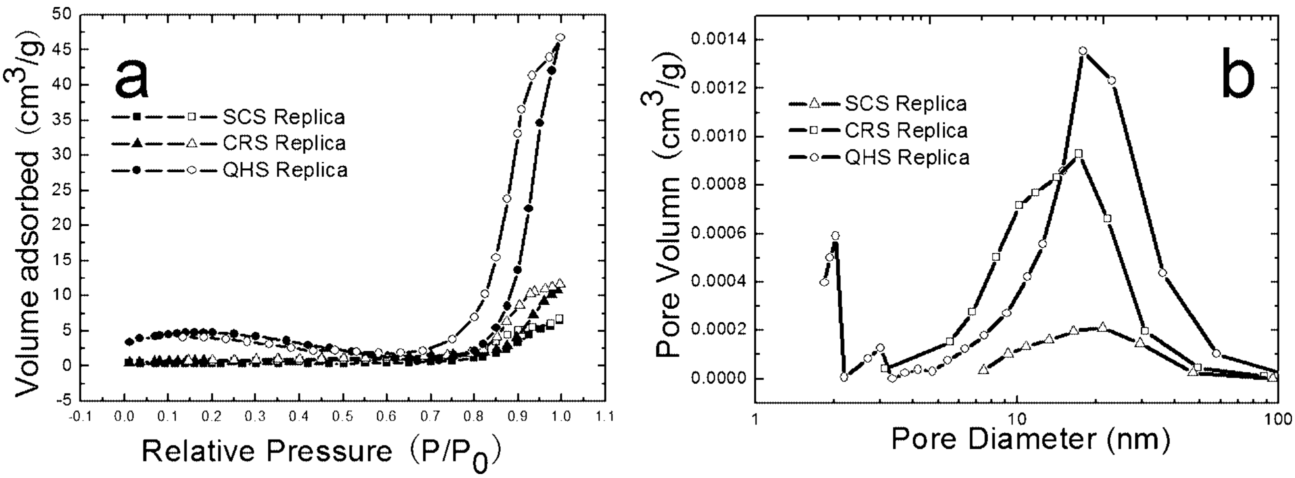

Figure 5. (a) Nitrogen adsorption−desorption isotherms; (b) the corresponding pore size distribution of the titania photoanodes with different butterfly wings structures.

Table 2. Pore Structural Parameters of Porous Materials Tested by N_2 Absorption−Desorption and Mercury Intrusion Porosimetry

measurements		samples		
methods	items	BU replica (shallow concaves)	BA replica (crossing ribs)	BA replica (quasi-honeycomb)
N_2 absorption−desorption measurements	BET area (m^2/g)	16.89	22.58	66.60
	pore volume (cm^3/g)	0.065	0.195	0.355
	mean pore diameter (nm)	15.4	18.5	23.8
mercury intrusion porosimetry	bulk density (g/cm^3)	1.9648	0.9647	0.6381
	apparent density (g/cm3)	4.3991	4.3321	4.3352
	porosity (%)	55.34	77.73	85.28
	mean pore diameter (μm)	0.1602	0.0457	0.0136
	total pore area (m^2/g)	1.335	5.299	21.694

column of Figure 1 shows. Figure S1 (see the Supporting Information) shows the whole nature picture of the male individual. The second level is the optical microscopy observation level, as images a and d in Figure 1 show. Figure 1a shows the area taken from the matte black wings of *Paplio paris*. The optical image (Figure 1d) is from the shining patch on the hind wings. The outline and color of the scales can be clearly identified in these images. FESEM was used to study the fine structures (the third and fourth level) of the wing scales. For FESEM measurement, all the samples were stuck to microscope stubs with double-sided carbon tape and then coated by a thin, sputtered gold layer to provide a conducting surface and avoid charging effects. It should be noted that previous studies[28] have proven that there is no significant distortion of the scale geometry during this process. The low-magnification images of the scales from blue and black areas on the wings are shown in images b and e in Figure 1. The scale morphologies are totally different, i.e., the blue shining scales (Figure 1e) on the patch presents one layer of scales with rounded endings, the arrangement of which on the wing resembles that of shingles on a roof. By contrast, the matte black scales (Figure 1b) are more elongated and have a deep zigzag ending, composed usually of three to five fingerlike features.

In this paper, we will focus on the fourth level, i.e., the surface and internal hierarchical structures of the scale,

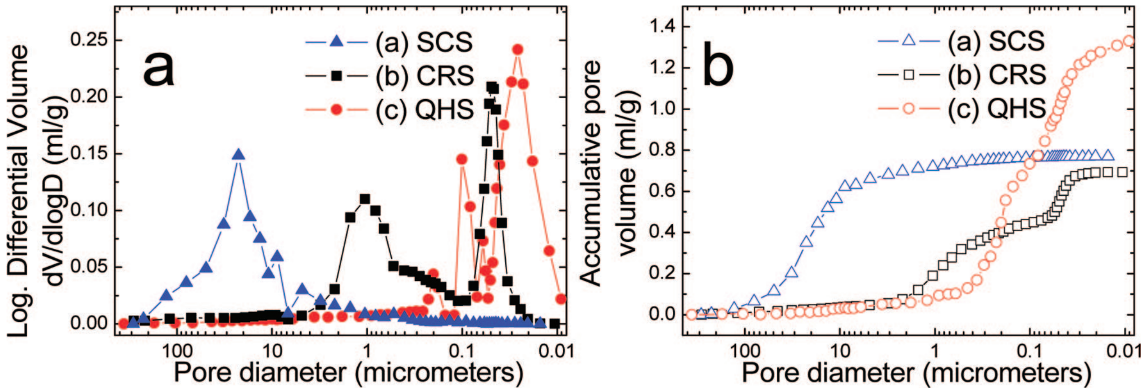

Figure 6. Pore size distribution of the TiO_2 anodes with different microstructures.

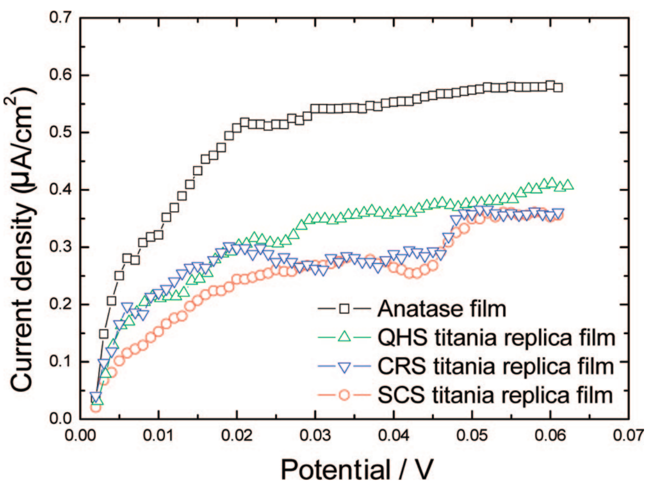

Figure 7. Current−potential curves of different microstructure photoanodes without dye sensitization.

because they are responsible for the structural colors of the wings. Medium-magnification FESEM images (images c and f in Figure 1) reveal that the structures of the blue and black scales have more obvious differences in the micron range. The black scales exhibit a complicated network structure called "quasi-honeycomb-like structure" (QHS), whereas the scanning electron micrographs of scales taken from the wings' blue patch regions show that their surfaces comprise a regular two-dimensional array of shallow concavities structure (SCS) of about 5 μm in width and 10 μm in length. These concaves are responsible for the blue coloration of male butterflies according to the similar research doing by P. Vukusic.[29]

To evaluate the morphology, especially the periodical distribution of spatial microstructure variation of the structures more quantitatively, two-dimensional logarithmic fast Fourier transform spectra of square areas selected from the images are shown as insets in images c and f in Figure 1. The measurements and statistics data, including average diameter, average hole area, and fill factor, etc., are compared in Table 1. The morphology differences are clearly observed in the Fourier power spectrum correspondingly. A diffuse elliptical ring pattern of Figure 1c indicates that the QHS has a regular arrangement, whereas a horizontal dotted line means the vertical longitudinal ridges. Figure S2 in the Supporting Information shows the standard FFT spectrum of beehive structures, which are a star-like pattern and more regular than the QHS in the butterfly wing scales. The spindle shape in Figure 1f shows the features attributed to the SCS, whereas the dotted line occurring in the first and third quadrant is due to the long ridges.

The as-synthesized titania photoanode microstructures were shown in Figure 2 with corresponding FFT images on the lower left-hand corner. The samples shown in the left column are synthesized in the lower concentration solution, while the right column samples are soaked in higher concentration. The morphology changes greatly, which are shown in the QHS (images a and b in Figure 2). In Figure 2b, the interspaces in the QHS are filled with titania particles, and the surface characters of the quasi-honeycomb structures are covered up. The changes are reflected on the corresponding FFT images, that is the diffuse ring pattern (shown in Figure 2a inset) disappeared in Figure 2b inset. By contrast, the spindle shape FFT from SCS are kept in the titania films, for the concavities are inherited in the titania films integrally, even the continued submicrometer drapes between the longitudinal ridges. The sizes of the samples before and after calcination are compared in Table 1. The fill factors are nearly the same except the full filled sample (QHS-2 replica). It means that the morphology characteristics are maintained well, which is corroborated by the FFT results shown in Figure 2.

TEM investigations of the fine quasi-honeycomb structure titania film were shown in Figure 3. The specimen was scraped from the titania replica film and smashed by ultrasonic. From TEM observation, the size and morphology of QHS was comparative to the FESEM results. The ridges of the replicas are a little thick, about 200 nm, which is out of the TEM resolution limits (50−100 nm); as such, the images are not quite clear. However, the outlines of the QHS still can be identified. The dotted white line in Figure 3b delineated the structure more clearly.

The transmission spectra measurements in the UV−vis range are shown in Figure 4a. The wing substrate and scales contain nearly the same amounts of pigments, especially the melanin, the differences in the transmission spectra are due to the diversity of the wings microstructures. The blue scales have higher transmissibility in longer wavelength, and the black ones with the CRS take second place, then the QHS ones take the third. According to the absorbance function

(28) Vukusic, P.; Sambles, J. R.; Lawrence, C. R. *Nature* **2000**, *403*, 36.
(29) Vukusic, P.; Sambles, J. R.; Lawrence, C. R. *Nature* **2000**, *404*, 457.

shown below, $A(\lambda) = 1 - R(\lambda) - T(\lambda)$, with $A(\lambda)$ being the absorbance, $T(\lambda)$ the transmittance, and $R(\lambda)$ the reflectance. For the black wing, reflectance is virtually constant throughout the whole spectral range. The QHS scales will have higher absorptivity than the CRS ones. Previous research[12] using scanning photodiode detector has approved this conclusion further both in air and in liquid bromoform. That is because the black scales from *Papilio paris* clearly comprise a more intricate and densely distributed lattice of cuticle than the scales appearing black in color from *Thaumantis diores* show. That is why the butterfly wings with QHS has a larger light absorption efficient than normal butterfly wings. Once the light incident to this structure, therefore, is more efficiently scattered than normal strucutures, a larger light absorption can be achieved.

The light harvest efficiency (LHE) of the photoanode was calculated by transmittance ($T\%$) and reflectance ($R\%$) using an integrating sphere (LHE(%) $= 100 - R\% - T\%$).[30] This formula was in agreement with the absorbance function given in the previous paragraph. So by comparing the absorbance of the titania replica films, the LHE can be evaluated. After calcination, the absorption spectra of the samples were collected and compared shown in Figure 4b. The absorbance values were converted from reflectance data by instrument based on the Kubelka−Munk theory. The absorption spectrum of the FTO glass substrate (red curve, in Figure 4b) was used as the background absorption in the whole measurements. After coating with a layer of anatase film using doctor blade methods, the curve shifted toward the longer wavelength due to the band-edge absorption of the titania. Three butterfly wing titania replicas with different microstructures (SCS, CRS, QHS) exhibited quite different absorption characteristics. The CRS titania replica film has a higher absorptivity than the normal anatase film in longer wavelength. The blue wings replica shows a lower absorptive peak around 450 nm, and as a result the film appeared a little yellow. It is heart-stirring that the QHS titania replica film has a remarkable increase in the absorption curve. Compared with the normal anatase film and CRS replica, the characteristic band-edge absorption position of the titania film with QHS is red-shifted to nearly 420 nm, because of the scatter and diffuse effect caused by the QHS in the titania replica film. This is similar to what happened in the original butterfly wings. Two main factors could influence the absorption spectra, one is the microstructures of the film, and the other is the remainder composing the film. All the samples were synthesized at the same condition, so the components of the film (TiO_2) would have the same properties, especially the crystal structures. To eliminate the possible influence, we took the EDXS analyses before and after fabrication. Investigation of original butterfly wings' chemical composition was taken by EDXS microanalysis. The results (see Figures S4 and S5 in the Supporting Information) show that the main elements are C and O. And the amounts of the other elements are very small less than 1 wt %. Also, the EDXS results of the as-synthesized photoanodes were given in Figure S6 (see the Supporting Information). The main elements of the samples are Ti and O. The replicas were sintered on the conductive surface of the FTO (SnO_2:F) and Sn signals were collected. And a little Na element came from the use of NaF in the fabrication process of the FTO. Within the experimental error of the EDXS, the compositions of the replicas were nearly the same. From all the above, we deduced that the microstructure differences in the photoanode are the main influencing factor of the absorption spectra differences.

Microstructure parameters of the titania films, such as surface area, pore size distribution, porosity, and particle size, greatly affect the photoelectric conversion efficiency of DSC modules, and the microstructure design and optimization of the mesoporous titania photoanode play an important role in the fabrication of high efficiency solar cells, for they have great influence on the dye adsorption and electrons transportation. Though the surface porosity, such as the pore size and fill factor, etc., can be estimated by the FESEM observation using IPP analysis, the inner pore properties are still unclear. N2 adsorption−desorption and mercury intrusion porosimetry (MIP) are two main physical methods to study the porous structure. MIP focused on larger pores, whereas N2 adsorption−desorption was good at microspore measurements. In this work, to study the titania film comprehensively, we involved both measurements and compared the results.

Figure 5 shows the nitrogen adsorption−desorption isotherm and the corresponding mesopore size distribution of the titania replica films with different microstructures, according to the Barrett−Joyner−Halenda (BJH) method.[31] The corresponding specific surface area, pore volume, and mean pore size diameter for the various corresponding titania replica samples prepared using different biotemplates are given in Table 2. BET specific surface areas greater than 66 m^2/g are obtained for the quasi-honeycomb microstructure butterfly wings, whereas for the BET specific surface areas are 22.58 and 16.89 m^2/g, respectively.

MIP results are shown in Figure 6 and Table 2. Figure 6 shows the pore diameter distribution of the porous materials. In Figure 6a, the experimental curves show the distribution of the pore diameter in terms of the ratio of pore volume at a specific pore diameter to the sample volume. In Figure 6b, the experimental curves show the distribution of the pore diameter in terms of the ratio of the sum of pore volume of pore diameter larger than a specific value to the sample volume. The most valued information that can be found in panels a and b in Figure 6 is the average diameter of the pores and the porosity, which are summarized in Table 2. Though the results are not exactly the same, trends in the changes of surface area and pore size distribution are nearly the same. It can be concluded that the QHS have the best surface area performance, which is very beneficial in enhancing the amount of dye adsorbed. The test shows that the pore distribution of the QHS titania film mainly range from 0.2 to 0.4 μm according to Figure 6b, which coincides with the TEM measurements shown in Figure 3. Furthermore, it is proved by the Rhodamine-B adsorption test,

(30) Sayama, K.; Nomura, A.; Zou, Z. G.; Abe, R.; Abe, Y.; Arakaw, H. *Chem. Commun.* **2003**, 2908.

(31) Barrett, E. P.; Joyner, L. G.; Halenda, P. P. *J. Am. Chem. Soc.* **1951**, *73*, 373.

shown in Figure S7 (see the Supporting Information). QHS has the best absorption amount compared to the titania photoanodes with the other microstructures.

Also, the electrical conductivity of the titania films was investigated as shown in Figure 7. In this case, normal anatase film has higher current than the other titania replica films. The lower current of the titania film replicas can be ascribed to the following two reasons. First, the titania replica films are sintered on the anatase film, so the thickness of these replica films is larger than the normal anatase film. A thicker film may decrease the electron transfer rate and therefore the current obtained. Second, the titania replica films are not very dense, so they did not have as good of connectivity as the anatase film made through the doctor-blade method. Transportation of electrons in the films may be baffled by the small windows or pores in the replicas. Therefore, all the current density of the QHS, CRS, and SCS replica films are lower than the normal anatase films. For all, the features are important and relevant in the DSC fabrication because, for example, the thickness increase will certainly reduce the titania electrical conductivity, whereas a larger surface area will enhance light and dye absorption. Moreover, the recombination and carrier scattering probabilities will be increased at the same time. So, to adjust the DSC efficiency, all the features of the DSC should be carefully balanced.

Conclusion

In conclusion, the butterfly wing scales templating procedure is a facile and economic design for the synthesis of hierarchically periodic microstructure titania photoanode without the need for complicated experimental conditions or equipments, such as photo lithography adopted. The quasi-honeycomb structure titania replica photoanode has a perfect light absorptivity and higher surface area, which give great advantages to the light harvesting efficiency and dye sorption. This structure gives the butterfly ultrablackness wings, so it is convincing that we could obtain potential ultra-absorptivity photoanode adopting the quasi-honeycomb structure. The successfully synthesized butterfly wing microstructure titania photoanode we obtained not only gives us new ideas to DSC researches in technology and theory but also opens a short cut to the photothermal, photocatalyzed, and photosensitized devices research. Also, the fabrication method may be applied to other chitin substrate template and metal oxide systems that could eventually lead to the production of optical, magnetic. or electric devices or components as building blocks for nanoelectronic, magnetic, or photonic integrated systems.

Acknowledgment. The authors express their thanks to the financial support of Program for National Basic Research Program of China (2006CB601200), National Natural Science Foundation of China (50671065), Major Fundamental Research Project of the Shanghai Science and Technology Committee (07DJ14001), New Century Excellent Talents in University (NCET-04-0387), and Shanghai Pujiang Program (06PJ14050).

Supporting Information Available: Nature image of the butterfly used. The sketch map of standard honeycomb structures and the corresponding FFT image. FESEM images of the original cross-ribbing structure (CRS) scale from *Thaumantis diores*. EDXS analyses of the original and titania replicas. UV−vis absorption spectra of different samples loading in RB solution at the same condition. This material is available free of charge via the Internet at http://pubs.acs.org.

CM702458P